

Nonequilibrium dynamics of the Hubbard dimer

Yaroslav Pavlyukh

Institute of Theoretical Physics, Faculty of Fundamental Problems of Technology,
Wroclaw University of Science and Technology, 50-370 Wroclaw, Poland
yaroslav.pavlyukh@pwr.edu.pl

Keywords: *Nonequilibrium Green's function theory, generalized Kadanoff-Baym Ansatz, excited states*

Electron dynamics in a two-sites Hubbard model is studied using the nonequilibrium Green's function approach. The study is motivated by the empirical observation that a full solution of the integro-differential Kadanoff-Baym equation (KBE) is more stable and often accompanied by artificial damping [Marc Puig von Friesen, C. Verdozzi, and C.-O. Almbladh (2009)] than its time-linear reformulations relying on the generalized Kadanoff-Baym ansatz (GKBA). Additionally, for conserving theories, numerical simulations suggest that KBE produces natural occupations bounded by one and zero in agreement with the Pauli exclusion principle, whereas, in some regimes, GKBA-based theories violate this principle. As the first step for understanding these issues, the electron dynamics arising in the adiabatic switching scenario is studied. Many-body approximations are classified according to the channel of the Bethe-Salpeter equation in which electronic correlations are explicitly treated. They give rise to the so-called second Born, T -matrix and GW approximations. In each of these cases, the model is reduced to a system of ordinary differential equations, which resemble equations of motion for a driven harmonic oscillator with time-dependent frequencies. A more complete treatment of electronic correlations is achieved by combining different correlation channels, with parquet theory serving as a starting point.

1 Introduction

Coherent electron dynamics in correlated materials attracts considerable attention due to the possibility of creating and controlling new quantum states by time-dependent perturbations [1]. Lattice systems such as the Hubbard model and its numerous extensions represent a versatile playground for testing many-body theories [2, 3, 4] and provide insight into the properties of correlated materials such as cuprates, transition metal oxides [5] and dichalcogenides [6].

Coherent dynamics in such systems can be launched by periodic field driving, quenching of system parameters with electric fields and in pump-probe experiments exploiting various combinations of phase-locked infrared (IR) and extreme ultraviolet (XUV) pulses. Coherent dynamics can be understood on the basis of the nonequilibrium Green's function (NEGF) approach, which can be applied perturbatively or combined with dynamical mean field theory. In a recent sequence of works [7, 8, 9] it has been demonstrated that numerical NEGF approach can be significantly accelerated by the use of the so-called generalized Kadanoff-Baym ansatz (GKBA) [10] which leads to the theory formulation in the form of coupled ordinary differential equations (GKBA+ODE).

The strength of GKBA+ODE lays in the possibility of various extensions [11, 12], such as the inclusion of electron-phonon interactions [13], multiparticle correlations [9], or transport [14]. It is also known that very systematic and balanced treatment of electronic correlations can be achieved by working not with self-energies, but rather with vertex functions. This gives rise to the so-called parquet method [15, 16], which combines correlations in the three channels: particle-particle (pp) and 2 particle-hole (ph , $p\bar{h}$).

In this work, I present the unexpected finding of exact analytic solutions for the Hubbard dimer separately in all three correlation channels within the NEGF+GKBA approximation and demonstrate the simplest possible way to combine the channels using the so-called fluctuating-exchange approximation (FLEX). Despite its simplicity, this model attracts recurrent attention in the pure electronic case [17, 18, 19, 20, 21], linearly [22, 23, 13] and quadratically [24] coupled with phonons, and can be studied experimentally as ultracold atoms in optical lattice systems [25].

The outline of the work is as follows. The GKBA+ODE approach is overviewed, presenting a uniform formulation for the three correlation channels. Next, it is demonstrated that the respective collision integrals can be combined together such that the double counting of Feynman diagrams can be avoided. Finally, analytic solutions for the driven Hubbard model using all aforementioned approximations are discussed.

2 Compendium of the GKBA+ODE scheme

Consider first a general form of the electronic Hamiltonian

$$\hat{H}(t) = \sum_{ij} h_{ij}(t) \hat{d}_i^\dagger \hat{d}_j + \frac{1}{2} \sum_{ijmn} v_{ijmn}(t) \hat{d}_i^\dagger \hat{d}_j^\dagger \hat{d}_m \hat{d}_n, \quad (1)$$

expressed in terms of fermionic operators $\hat{d}_i^\dagger, \hat{d}_j$, where i may stand for spatial degrees of freedom and spin. In the NEGF formalism the fundamental unknowns are the electronic lesser/greater single-particle Green's functions

$$G_{ij}^<(t, t') = i \langle \hat{d}_j^\dagger(t') \hat{d}_i(t) \rangle, \quad G_{ij}^>(t, t') = -i \langle \hat{d}_i(t) \hat{d}_j^\dagger(t') \rangle, \quad (2)$$

They satisfy the Kadanoff-Baym equations of motion, which are mathematically integro-differential equations:

$$[i\partial_t - h_e(t)] G^{\lessgtr}(t, t') = [\Sigma^{\lessgtr} \cdot G^A + \Sigma^R \cdot G^{\lessgtr}](t, t'), \quad (3)$$

where $[A \cdot B](t, t') \equiv \int d\bar{t} A(t, \bar{t}) B(\bar{t}, t')$, is a real-time convolution and $X^{R/A}(t, t')$ are the retarded/advanced functions, and Σ is the correlation part of the self-energy. We work in zero-temperature formalism, therefore contributions due to vertical track of the Keldysh contour are not included in Eq. (3). The time-local mean-field part is incorporated into the Hartree-Fock Hamiltonian $h_{\text{HF},ij}(t) = h_{ij}(t) + \sum_{mn} w_{imnj} \rho_{nm}^<(t)$ with $w_{imnj} = v_{imnj} - v_{imjn}$, and we also introduced densities according

$$\rho_{ij}^{\lessgtr}(t) = -i G_{ij}^{\lessgtr}(t, t). \quad (4)$$

By combining Eq. (3) with its adjunct and going to the equal times limit one obtains:

$$\frac{d}{dt} \rho^<(t) = -i [h_{\text{HF}}(t), \rho^<(t)] - (I(t) + I^\dagger(t)). \quad (5)$$

The collision term can be expressed in terms of the two-particle Green's function (2-GF)

$$I_{lj}(t) = -i \sum_{imn} v_{lnmi}(t) \mathcal{G}_{imjn}(t). \quad (6)$$

Eq. (5) is not closed because the $\mathcal{G}_{imjn}(t)$ can be expressed as a functional of the two-times Green's function $G_{ij}^<(t, t')$. The complicated time-dependence in $G_{ij}^<(t, t')$ is decoupled with the help of GKBA

$$G^{\lessgtr}(t, t') = -G^R(t, t') \rho^{\lessgtr}(t') + \rho^{\lessgtr}(t) G^A(t, t'), \quad (7)$$

whereby using a simpler form of the retarded propagator:

$$G^R(t, t') = -i \theta(t - t') T \left\{ e^{-i \int_{t'}^t d\tau h_{\text{HF}}(\tau)} \right\}. \quad (8)$$

Let us consider now a large class of approximations in which 2-GF is given as a solution of the one-channel Bethe-Salpeter equation. Depending on the channel in which electronic correlations are treated, pp , ph or \overline{ph} , they are known as T -matrix and GW approximations. For Hubbard models, the cancellation of direct and exchange diagrams for electrons with equal spin also allows to formulate the second Born approximation as the common leading term of all three methods, and it can be treated on equal footing.

A particularly concise formulation is achieved by introducing matrix notations [9] for rank-4 tensors like 2-GF \mathcal{G} , Coulomb interaction \mathbf{v} , and the response-functions: the full $\boldsymbol{\chi}$ and the noninteracting $\boldsymbol{\chi}^0$ ones. The index order is different for each approximation as summarized in Tab. 1. The one-time $\mathcal{G}(t)$ can be represented then as

$$\mathcal{G}(t) = -i \int_0^t dt' \left\{ \boldsymbol{\chi}^>(t, t') \mathbf{v}(t') \boldsymbol{\chi}^{0,<}(t', t) - (\rightarrow \leftrightarrow \leftarrow) \right\}, \quad (9)$$

Table 1: Definitions of electronic two-particle tensors. The vertically grouped indices are combined into one super-index.

Quantity	2B and GW	T^{pp}	T^{ph}
$i\chi_{24}^{0,\lessgtr}(t, t')$	$G_{13}^{\lessgtr}(t, t')G_{42}^{\gtrless}(t', t)$	$-G_{13}^{\lessgtr}(t, t')G_{24}^{\lessgtr}(t, t')$	$-G_{13}^{\lessgtr}(t, t')G_{42}^{\gtrless}(t', t)$
$\mathcal{G}_{24}^{13}(t)$	$\mathcal{G}_{4132}(t)$	$\mathcal{G}_{1234}(t)$	$\mathcal{G}_{1432}(t)$
$\mathbf{h}_{24}^{13}(t)$	$h_{13}\delta_{42} - \delta_{13}h_{42}$	$h_{13}\delta_{24} + \delta_{13}h_{24}$	$h_{13}\delta_{42} - \delta_{13}h_{42}$
$\mathbf{v}_{24}^{13}(t)$	$v_{1432}(t)$	$v_{1243}(t)$	$v_{1423}(t)$
$\rho_{24}^{\lessgtr}(t)$	$\rho_{13}^{\lessgtr}(t)\rho_{42}^{\gtrless}(t)$	$\rho_{13}^{\lessgtr}(t)\rho_{24}^{\lessgtr}(t)$	$\rho_{13}^{\lessgtr}(t)\rho_{42}^{\gtrless}(t)$

Here χ is the response function describing the pure electronic screening in the respective channel. In Fig. 1, the representation is illustrated for the GW case in application to the Hubbard model. By differentiating Eq. (9) with respect to time one obtains the following equation of motion

$$i\frac{d}{dt}\mathcal{G}(t) = -\Psi(t) + [\mathbf{h}(t) + a\rho^\Delta(t)\mathbf{v}(t)]\mathcal{G}(t) - \mathcal{G}(t)[\mathbf{h}(t) + a\mathbf{v}(t)\rho^\Delta(t)], \quad (10)$$

where \mathbf{h} is effective two-particle Hamiltonian. Other ingredients are defined as

$$\rho^\Delta(t) \equiv \rho^>(t) - \rho^<(t), \quad (11)$$

$$\Psi(t) \equiv \rho^>(t)\mathbf{v}(t)\rho^<(t) - \rho^<(t)\mathbf{v}(t)\rho^>(t), \quad (12)$$

where ρ^{\lessgtr} and the lesser/greater two-particle densities. Constant a is method-dependent and is equal to 0, -1 and 1 for second Born, GW and T -matrix approximations, respectively.

3 Application to the Hubbard dimer

Specifying Eq. (1) to the site-spin basis $i \equiv (\mathbf{i}, \sigma_i)$, restricting to the nearest neighbors ($\langle \mathbf{i}, \mathbf{j} \rangle$) hopping $h_{i\sigma_i j\sigma_j} = h\delta_{\langle \mathbf{i}, \mathbf{j} \rangle \delta_{\sigma_i \sigma_j}}$, and setting

$$v_{i\sigma_i j\sigma_j k\sigma_k l\sigma_l} = U\delta_{ij}\delta_{kl}\delta_{jk}\delta_{\sigma_i \sigma_l}\delta_{\sigma_j \sigma_k}, \quad (13)$$

one obtains the Hubbard Hamiltonian

$$\hat{H}_H = \hat{T} + \hat{H}_U = h \sum_{\sigma} \sum_{\langle \mathbf{i}, \mathbf{j} \rangle} \hat{d}_{i\sigma}^\dagger \hat{d}_{j\sigma} + U \sum_{\mathbf{i}} \hat{n}_{i\uparrow} \hat{n}_{i\downarrow}, \quad (14)$$

where h is the hopping parameter, and U is the on-site repulsion and $\hat{n}_{i\sigma} = \hat{d}_{i\sigma}^\dagger \hat{d}_{i\sigma}$. In what follows, I will focus on the case where a lot of progress can be done analytically: the half-filled two-site Hubbard model ($N = 2$ and $\sum_{\mathbf{i}} \langle \hat{n}_{i\sigma} \rangle = 1$). This system has a large number of symmetries ($D_{\infty h}$ point group). From the translational invariance follows that all physical operators are given by Toeplitz matrices. In particular, the one-body Hamiltonian in the site basis is represented as a matrix

$$T = \begin{pmatrix} 0 & h \\ h & 0 \end{pmatrix}, \quad \text{or for brevity } T = [0 \quad h]. \quad (15)$$

Other symmetries (reflections) impose further restrictions on the density matrix: it is not only Hermitian, but also symmetric and can be written in terms of just one parameter (site basis, using shorthand notation for Toeplitz matrices)

$$\rho_{\sigma} = [1/2 \quad a]. \quad (16)$$

The Hartree-Fock Hamiltonian with this density reads

$$h_{\text{HF}} = [U/2 \quad h], \quad (17)$$

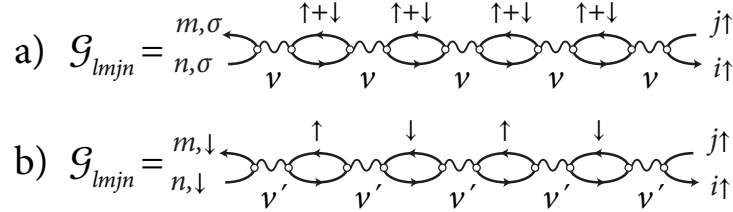


Figure 1: Diagrammatic representation of the 2-GF (GW approximation) for two forms of the Coulomb interaction in the Hubbard model.

with the eigenvalues

$$\epsilon_i^{\text{HF}} = U/2 \pm h. \quad (18)$$

Density matrix based on the lowest energy eigenvector of Hamiltonian (17) then reads

$$\rho_\alpha^{\text{HF}} = [1/2 \quad -1/2]. \quad (19)$$

Consider now the driving protocol in which $U = U(t)$ and $h = 1$, and the density matrix possesses the full symmetry of the system at every time instance. This discards the possibility of spontaneous dimerization. In such a scenario the density matrix in site basis can *always* be written in the form (16) with a time-dependent parameter $a(t)$. This means that HF Hamiltonian has always the same eigenvectors, but time-dependent eigenvalues (18) (via parametric dependence of U on time). Thus, HF basis is fixed. HF-Hamiltonian is time-dependent and diagonal in this basis. Likewise, the density matrix is time-dependent and diagonal. Since diagonal matrices commute $[h_{\text{HF}}(t), \rho_\sigma(t)] = 0$, in our driving protocol the density matrix is driven exclusively by the collision term

$$\dot{a}(t) = -2U(t)\Phi_2(t), \quad (20)$$

where $\Phi_m(t) = -i\mathcal{G}_{11m1}(t)$ is introduced, and the initial condition according to Eq. (19) reads

$$a(t_i) = -1/2. \quad (21)$$

Now the equations of motion for matrix elements of 2-GF for various approximations will be formulated and analysed.

Second Born approximation The EOM for $\Phi_2(t)$ follows from Eq. (10). After long but trivial calculations one obtains that 2-GF fulfills a *driven oscillator equation*

$$\ddot{\Phi}_2(t) + 16\Phi_2(t) = \dot{L}(t). \quad (22)$$

with the time-dependent driving

$$L(t) = U(t)(a(t)^3 + \frac{1}{4}a(t)) \equiv U(t)\lambda(t). \quad (23)$$

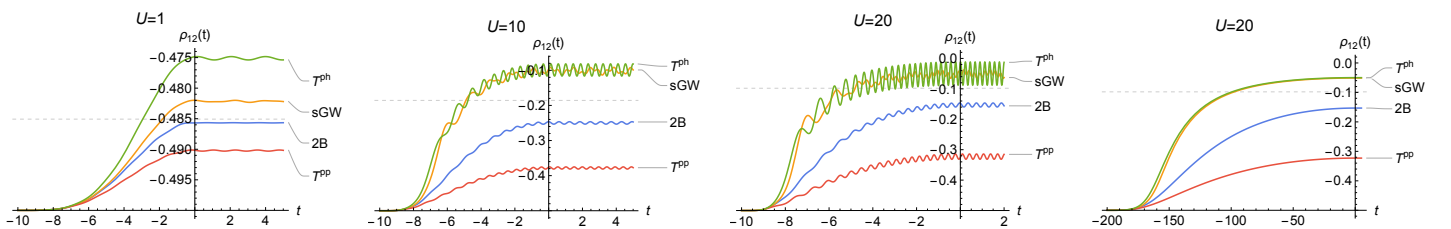


Figure 2: The GKBA thermalization of the Hubbard dimer computed using exact equations for different correlated methods. It is quite surprising that T^{ph} and sGW produce very different results for small- U , whereas the two methods asymptotically converge to the same value for $U \rightarrow \infty$. Exact thermalized values determined by Eq. (33) are shown as dashed lines.

T -matrix approximations A marked feature of these correlated methods is that the oscillator eigenfrequency in Eq. (22) becomes modulated by the single-particle density. Introducing

$$K(t) = U(t)a(t), \quad (24)$$

one obtains two coupled oscillators equations

$$\ddot{\Phi}_2(t) + 16(1 \pm K(t))\Phi_2(t) = \dot{L}(t) \pm 2\dot{K}(t)\Phi_1(t), \quad (25a)$$

$$\dot{\Phi}_1(t) = -4\Phi_2(t), \quad (25b)$$

where the upper and lower signs correspond to the ph and pp channels, respectively. The initial conditions are

$$\Phi_m(t_i) = \dot{\Phi}_m(t_i) = 0. \quad (26)$$

GW approximation Eq. (13) yields the Hubbard interaction $Un_{i\uparrow}n_{i\downarrow}$ only in conjunction with the Pauli principle. However, it is not guaranteed when working perturbatively that the only scattering processes are those between the particles of opposite spin, Fig. 1(a). In this example the intermediate fermionic bubbles may carry arbitrary spin leading to overscreening. Same-spin scattering can be eliminated by introducing a spin-dependent interaction [3, 26]

$$v'_{i\sigma_i j\sigma_j k\sigma_k l\sigma_l} = v_{i\sigma_i j\sigma_j k\sigma_k l\sigma_l}(1 - \delta_{\sigma_i\sigma_j}). \quad (27)$$

leading to 2-GF in Fig. 1(b). This method will be called spin- GW or sGW . Corresponding 2-GF equation (10) becomes more involved due to the necessity of considering correlators with two different spin-orders that for brevity are denoted as $a = \uparrow\downarrow\uparrow\downarrow$ and $b = \uparrow\uparrow\uparrow\uparrow$:

$$\ddot{\Phi}_2^a(t) + 16\Phi_2^a(t) = -2\dot{K}(t)\Phi_1^b + 16K(t)\Phi_2^b + \dot{L}(t), \quad (28a)$$

$$\ddot{\Phi}_2^b(t) + 16\Phi_2^b(t) = -2\dot{K}(t)\Phi_1^a + 16K(t)\Phi_2^a, \quad (28b)$$

$$\dot{\Phi}_1^a(t) = -4\Phi_2^a(t), \quad (28c)$$

$$\dot{\Phi}_1^b(t) = -4\Phi_2^b(t). \quad (28d)$$

Notice that the driving term is present only for the mixed spin component, which now enters the density equation (20).

To summarize, the EOM for the density matrix (5) is reduced to a single differential equation (20) for a single off-diagonal element. The EOM for 2-GF (10) takes different form depending on the approximation: Eq. (22) (2B), Eq. (25) (T -matrix), and Eq. (28) (sGW) (see Supplemental Information for detailed derivations). Numerical solutions of these equations for the adiabatic switching protocol

$$U(t) = \begin{cases} U \sin^2\left(\frac{\pi}{2}\frac{(t+\tau)}{\tau}\right) & \tau < t < 0, \\ U & t \geq 0; \end{cases} \quad (29)$$

and different final Hubbard- U and switching times ($t_i = \tau$) are shown in Fig. 2. There are two observations in comparison with earlier works using the full KBE propagation. First of all, a crucial difference between the GKBA method and the full solution of KBE is that the former does not lead to the artificial damping observed in the paper of Marc Puig von Friesen, C. Verdozzi, and C.-O. Almbladh [2]. Besides the numerical evidences, this observation is supported by the structure of the obtained equations, which have a driven oscillator form without a damping term. The damping was discussed in another papers by the same authors [3, 27], and a plausible explanation is that it results from self-consistent treatments, leading to an infinite number of poles in the electron Green's function. In contrast, an exact solution should only have a finite number of poles for finite systems. Another interesting effect is the lack multiple steady states [2, 3]. This is also an artefact of exact calculation not observed in the GKBA scheme. As comparison of Fig. 2(c) and (d) shows, fast switching of the interaction leads to oscillations, but there is never a transition to a state different from the one obtained by slow adiabatic switching. This holds true even when artificial damping term is added. However, it is not possible to exclude that under some combination of parameters an artificial steady state can be reached.

3.1 Asymptotic analysis

Starting from the zero-temperature adiabatic assumption the correlated density matrix of the ground state of the system can be determined analytically for 2B and T -matrix methods. To this end equations of motion are written in the form common to all methods, the $\ddot{\Phi}_2(t)$ is neglected assuming infinitesimally slow switching, parametric dependence of physical quantities on U is introduced, i.e., $a(U) \equiv a(U(t))$, and $f(u) \equiv \Phi_1(U(t))$. We obtain

$$2D_U[a(U)] = UD_U[f(U)], \quad (30a)$$

$$-4D_U[f(U)](1 - a(U)\eta U) = D_U[u\lambda(a(U))] - 2\eta f(U)D_U[Ua(U)], \quad (30b)$$

$$a(0) = -1/2, f(0) = 0. \quad (30c)$$

where $\eta = 1, -1, 0$ for T^{pp} , T^{ph} , 2B approximations, respectively. D_U denotes the derivative with respect to U and $\lambda(a) = a^3 + \frac{1}{4}a$. Surprisingly, these equations can be analytically integrated (see Supplemental Information for detailed derivations) leading to

$$a^2 \left[16 + 16(1 + 4a^2) + U^2(1 + 4a^2)^2 \right] = 12, \quad 2B; \quad (31a)$$

$$a^2(Ua + 2)^2 = Ua + 1, \quad T^{ph}; \quad (31b)$$

$$a(a(Ua - 2)^2 + U) = 1, \quad T^{pp}. \quad (31c)$$

The derivation for the spin GW method proceeds along the same line, except there are more equations to solve. As the consequence, it is not possible to integrate all of them. However, one can reduce (Supplemental Information) them to a single nonlinear ordinary differential equation

$$p(a, U)a'(U)^2 + q(a, U)a'(U) + r(a, U) = 0, \quad (32)$$

where

$$\begin{aligned} p(a, U) &= 3U^2a^2(36U^4a^4 + 3(U^2 - 48)U^2a^2 - U^4 + 8U^2 + 192) - (U^2 + 16)^2, \\ q(a, U) &= 2Ua(9U^4a^4 - 3U^2(U^2 - 4)a^2 - (U^2 + 16)), \\ r(a, U) &= U^2a^2(3U^2a^2(3a^2 - 1) - 1). \end{aligned}$$

While we were not able to solve Eq. (32) analytically, it is possible to perform series expansions and to compare with the exact solution [28] that has much simpler form

$$a(U) = -\frac{2}{\sqrt{U^2 + 16}}. \quad (33)$$

From the implicit equations (31), differential equation (32) and algebraic equation (33) we obtain the series expansions for $U \rightarrow 0$

$$a = -\frac{1}{2} + \frac{U^2}{64} - \frac{3U^4}{2048} + \mathcal{O}(U^6), \quad 2B; \quad (34a)$$

$$a = -\frac{1}{2} + \frac{U^2}{64} + \frac{9U^4}{4096} + \mathcal{O}(U^6) \quad sGW; \quad (34b)$$

$$a = -\frac{1}{2} + \frac{U^2}{64} + \frac{U^3}{128} + \frac{9U^4}{4096} + \mathcal{O}(U^6), \quad T^{ph}; \quad (34c)$$

$$a = -\frac{1}{2} + \frac{U^2}{64} - \frac{U^3}{128} + \frac{9U^4}{4096} + \mathcal{O}(U^6), \quad T^{pp}; \quad (34d)$$

$$a = -\frac{1}{2} + \frac{U^2}{64} - \frac{3U^4}{4096} + \mathcal{O}(U^6), \quad \text{exact}. \quad (34e)$$

All of them are exact of to the second order. This is expected because the second order diagrams are fully taken into account by all the methods. T -matrix methods contain terms of the thirds order corresponding to the ladder diagrams with three interaction lines. Exact result does not have these terms.

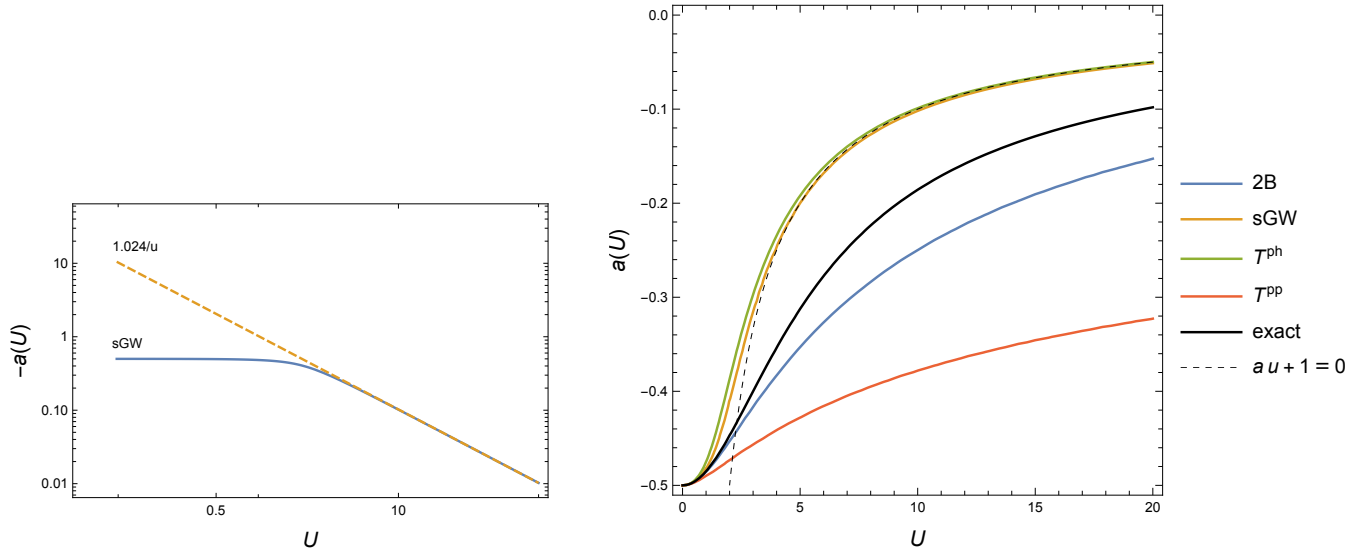


Figure 3: Asymptotics of the off-diagonal density matrix element $a(U)$ for the spin- GW method (left) and comparison of $a(U)$ for different methods (right).

Thus, these diagrams must be compensated by other third order diagrams not accessible with our method. The spin GW method contains only the even order terms. This is expected from the diagrammatic construction illustrated in Fig. 1. 2B method also contains only even order terms. Terms of fourth order and higher arise from the self-consistent solution of the Dyson equation.

For large values of U the off-diagonal density approaches zero as

$$a = -\frac{2\sqrt{3}}{U} + \mathcal{O}(U^{-3}), \quad 2B; \quad (35a)$$

$$a = -\frac{1.024}{U} + \mathcal{O}(U^{-3}), \quad sGW; \quad (35b)$$

$$a = -\frac{1}{U} + \mathcal{O}(U^{-3}), \quad T^{ph}; \quad (35c)$$

$$a = -\frac{1}{U^{1/3}} + \frac{1}{U} + \mathcal{O}(U^{-3}), \quad T^{pp}; \quad (35d)$$

$$a = -\frac{2}{U} + \mathcal{O}(U^{-3}), \quad \text{exact}. \quad (35e)$$

It is quite unexpected that T^{pp} approximation fails to provide even the $-1/U$ asymptotic dependence of the exact solution. It should also be noticed that spin- GW is numerically very close to the T^{ph} method, however, the asymptotic coefficient (determined numerically) is slightly different [-1.024 , see Fig. 3(left)]. This indicates that physically the two methods are physically different, and the observed similarity is rather a coincidence.

Analysing further the $a(U)$ dependence based on Eqs. (31) allows to conclude that physical (fulfilling the initial condition) branch of the considered theories always satisfies $-1/2 < a(U) \leq 0$ in equilibrium. This indicates that natural occupations $n_i(U)$ are always in the range $0 \leq n_i \leq 1$, as stipulated by the Pauli exclusion principle. This is a non-trivial finding as apart from the Hartree-Fock approximation there is no proof that the natural occupations should adhere to physical limits in correlated theories treated within GKBA. In fact, there are electronic [21] and electron-phonon [12] systems, where under some conditions violations of these limits occur.

It is also interesting to note that the structure of time-dependent equations (25) is very similar to the structure of electron self-energies derived for the same system in the ground state [29]. For instance for T^{ph} and T^{pp} , the self-energy poles (see Eqs.(53, 43) therein) are expressed in terms of the effective Hamiltonian that reduces to the double effective frequency in Eq. (25) ($\Omega^2 = 1 \pm aU$) when Hartree-Fock $a = -1/2$ is used therein. It also explains why the T^{ph} theory of Ref. [29] is unstable when U approaches

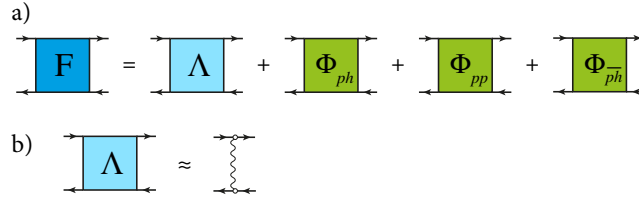


Figure 4: (a) Vertex function as a sum of irreducible and two-particle reducible correlators, Eq. (36). (b) Approximation of the lowest-order irreducible vertex by the direct Coulomb interaction (exchange is not included).

2, and why such an instability is absent in our case. As can be seen from Fig. 3(right), in our approach a depends on U and therefore the effective frequency $1 + aU$ (dashed line) never becomes equal to zero.

4 Combining channels

Numerical examples shown above indicate that sGW , T^{pp} and T^{ph} approximations, despite containing infinite sequence of Feynman diagrams via the solution of the Bethe-Salpeter equation in the respective channels, are describing physically very different scenarios. Can one exploit the advantages of each approximation? In the following, I derive such an approximation starting from the exact parquet equations [16]. This derivation is complementary to the self-energy based derivation in Ref. [30]. The motivation for this starting point is two-fold: on one side this derivation establishes that there is no double counting of Feynman diagrams. On the other side, it demonstrates difficulties of going beyond. They are associated with multiple time-arguments of constituent vertex functions [31]. In particular, working in one channel allows one to express the one-time 2-GF in terms of two-times response functions, see for instance Eq. (28) of Ref. [9], and to close the equation of motion for it. Combining the channels requires in general to deal with 4-times quantities for which GKBA is not known.

Consider the full (reducible) vertex \mathbf{F} , which is just 2-GF with amputated fermionic lines, i. e., $i\mathcal{G} = \chi^0 \mathbf{F} \chi^0$. This equation is written schematically as it does not reflect the time arguments of the ingredients. Reducing \mathcal{G} to two-times form is the main goal here. Quite generally, the *vertex* function \mathbf{F} can be written as a sum of the *fully irreducible vertex* Λ and reducible vertices Φ_i

$$\mathbf{F} = \Lambda + \sum_i \Phi_i, \quad (36)$$

where $i = pp, ph, \overline{ph}$ denotes the channels, in which Φ_i are *two-particle reducible*. Eq. (36) is, therefore, only a topological statement (Fig. 4). It is important because it rules out any double counting of the resulting Feynman diagrams.

The reducible vertices Φ_i fulfill a set of interrelated equations (see first line of Fig. 5 for the exact equation in the ph channel). Two approximations can be introduced allowing to transit from four to two time-arguments: (i) The leading term for each equation is written as $(\mathbf{F}\chi^0\Lambda)_i$ (second line of Fig. 5) in all channels. Here, the subscript i indicates that quantities in the brackets are given in the index order pertinent to the channel, other terms are discarded; (ii) Approximating therein

$$\mathbf{F} \approx \Lambda + \Phi_i, \quad (37)$$

(third line) and using $\Lambda \approx \mathbf{v}$ [Fig. 4(b)] leads to the Bethe-Salpeter equation for the two-particle reducible functions (forth line of Fig. 5)

$$\Phi_i(z, z') \approx \mathbf{v}(z)\chi_i^0(z, z')\mathbf{v}(z') + \int_{\mathcal{C}} d\bar{z} \Phi_i(z, \bar{z})\chi_i^0(\bar{z}, z')\mathbf{v}(z'), \quad (38)$$

where z, z' are times on the Keldysh contour \mathcal{C} . χ_i^0 is written explicitly for each channel in Tab. 1, where GW approximation corresponds to the treatment of \overline{ph} channel, T^{pp} approximation — pp channel, and T^{ph} — ph channel. Notice that while exact Bethe-Salpeter equations are formulated for 4-times correlators, the final approximated equation is closed for Φ_i dependent on two-times.

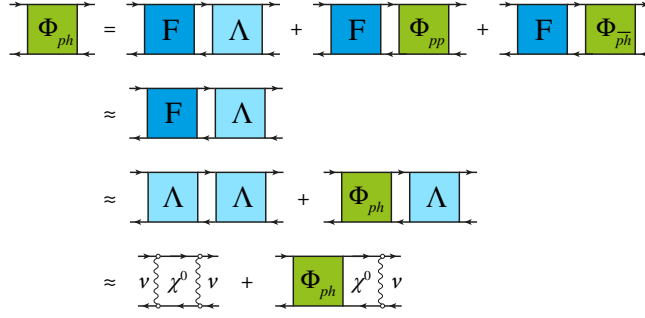


Figure 5: Derivation of the Bethe-Salpeter equation (38) for the two-particle ph reducible correlator. \overline{ph} and pp channels are treated in the same way. Notice that the first approximation means setting the irreducible vertex in the ph channel to the fully irreducible vertex (and similarly in other channels). This is exactly what defines the FLEX approximation [32].

Decorating Φ_i with χ_i^0 on both sides of Eq. (38) one obtains the RPA equations for the full response functions $\chi_i(z, z')\mathbf{v}(z') = [\chi_i^0 \cdot (\mathbf{v} + \Phi_i)](z, z')$:

$$\chi_i(z, z') = \chi_i^0(z, z') + \int_{\mathcal{C}} d\bar{z} \chi_i(z, \bar{z})\mathbf{v}(\bar{z})\chi_i^0(\bar{z}, z'). \quad (39)$$

Let us now decorate the vertex functions in Eq. (37) with four fermionic lines and go to the equal time-limit (t) for the external time-arguments

$$i\mathcal{G}_i(t) = [\chi_i^0 \cdot \mathbf{v} \cdot \chi_i^0 + \chi_i^0 \cdot \Phi_i \cdot \chi_i^0](t) = [\chi_i \cdot \mathbf{v} \cdot \chi_i^0](t). \quad (40)$$

In this way Eq. (9) was re-derived for each channel. However, one can do better by using the *full* vertex as in Eq. (36) instead of the *partial* vertex as in Eq. (37). To this end, let us decorate Eq. (36) ($\Lambda \approx \mathbf{v}$) with four fermionic lines with equal external time-arguments (t). It follows then

$$\mathcal{G}(t) = -2\mathcal{G}_{2B}(t) + \sum_i \mathcal{G}_i(t). \quad (41)$$

Notice that the matrix notations (Tab. 1) are not used here because each approximation has own order of indices. Instead, \mathcal{G} s are interpreted here as usual rank-four tensors, like in Eq. (6). A crucial point of this derivation is to realize that

$$i\mathcal{G}_{2B}(t) = [\chi_i^0 \cdot \mathbf{v} \cdot \chi_i^0](t) \quad (42)$$

is independent on the channel i and is given simply by the second Born approximation for 2-GF. This can be verified by using definitions in Tab. 1 (provided that lhs of this equation is written with index order pertinent to the rhs). Therefore Eq. (41) can be written explicitly for the Hubbard model with spin-dependent interactions (27) as

$$\mathcal{G}_{\text{FLEX}}(t) = -2\mathcal{G}_{2B}(t) + \mathcal{G}_{sGW}(t) + \mathcal{G}_{Tpp}(t) + \mathcal{G}_{Tph}(t). \quad (43)$$

The resulting approximation is denoted as FLEX—the fluctuating-exchange approximation—which seems to be the common term [33, 34, 8]. It may be viewed as a first-order element in a hierarchy of successive approximations to the full parquet solution [35, 32].

Thermalization is possible only for small values of U as depicted in Fig. 6 (left). There is, however, a simple procedure that stabilizes the GKBA+ODE methods. It was already mentioned that EOMs for the matrix elements of 2-GF have a driven harmonic oscillator form, viz. Eq. (22, 25, 28). By introducing a “velocity damping” with coefficient k (see Supporting Information for the exact form of equations) converged solutions can be obtained even for strongly correlated cases, Fig. 6 (right). If for a given method the adiabatic switching procedure can be performed, then the final density matrix of the system is characterised by the $a(U)$ value independent of a small damping k . The term “small” stipulates that the magnitude of damping should not exceed other energy scales in the system (see Supporting Information for the investigation of the role of k). While the “damping” approach work excellently for

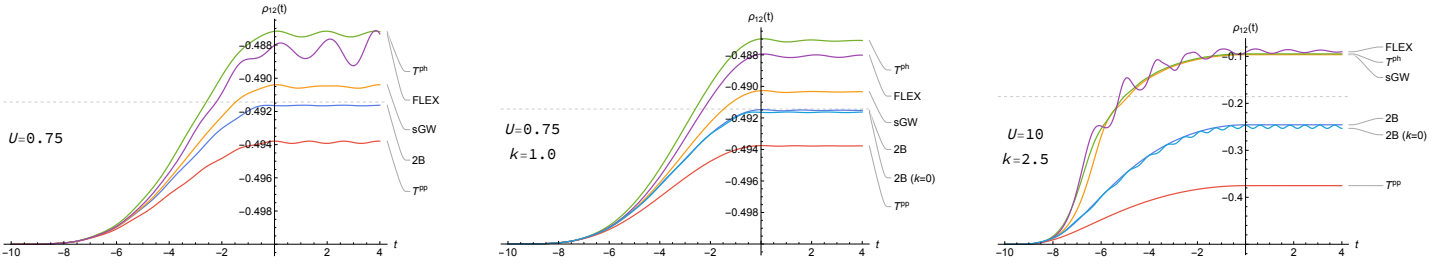


Figure 6: The GKBA thermalization of the Hubbard dimer computed using exact equations for different correlated methods. Dashed horizontal line depicts exact thermalized value of $a(t)$ given by Eq. (33).

the Hubbard dimer, further work is needed in order to generalize this approach to more complicated systems.

Finally, we remark that our approach is different from the dynamically-screened-ladder approximation in Ref. [8] in that four ingredient 2-GFs in Eq. (43) are independently propagated.

5 Conclusions and outlook

Exact many-body electron dynamics in a finite basis representation is described by the linear differential equation for the wave-function. Reformulations of this dynamics on the language of reduced quantities, such as nonequilibrium Green's functions, inevitably lead to the equations of motion with much more complicated mathematical structure. One of the first attempts to analyze the integro-differential Kadanoff-Baym equations in this perspective have been made by Marc Puig von Friesen, C. Verdozzi, and C.-O. Almbladh [3]. They have made a number of interesting observations concerning non-unique steady states and the role of the correlation-induced damping. These findings are revisited here in view of the rapid development of the time-linear methods that can be formulated as a system of coupled ordinary differential equations. In this work, the first steps are taken in the investigation of the nonlinear form of the GKBA+ODE scheme by applying it to the two-sites Hubbard model. This involves deriving oscillator-like equations for the components of the two-particle GF and analyzing the adiabatic switching scenario and the steady-state limit. This has led to the observation of similarities between equations in different channels, systematic under- and over-estimations of the correlational effects pertinent to different schemes and very close but distinct asymptotic limits for the T^{ph} and sGW methods. It was also possible to prove analytically that second Born, T -matrix and spin- GW approximations never violate the Pauli exclusion principle in the steady state limit. Nonetheless, such violations may take place under strongly nonequilibrium conditions. Further investigations of these effects are needed. The structure of the GKBE+ODE equations in the dimer case hints that this is a challenging mathematical problem.

Supporting Information

Supporting Information is available from the Wiley Online Library or from the author.

Acknowledgements

I would like to thank Enrico Perfetto and Gianluca Stefanucci for insightful discussions, and Hugo U.R. Strand, Claudio Verdozzi, Michael Bonitz for the excellent organization of the PNGF8 conference. This research was part of project no. 2021/43/P/ST3/03293 cofunded by the National Science Centre and the European Union's Horizon 2020 research and innovation programme under the Marie Skłodowska-Curie grant agreement no. 945339.

References

- [1] D. N. Basov, R. D. Averitt, D. Hsieh, *Nat. Mater.* **2017**, *16*, 11 1077.
- [2] M. P. von Friesen, C. Verdozzi, C.-O. Almbladh, *Phys. Rev. Lett.* **2009**, *103*, 17 176404.
- [3] M. Puig von Friesen, C. Verdozzi, C.-O. Almbladh, *Phys. Rev. B* **2010**, *82*, 15 155108.
- [4] D. Karlsson, A. Privitera, C. Verdozzi, *Phys. Rev. Lett.* **2011**, *106*, 11 116401.
- [5] K. Gillmeister, D. Golež, C.-T. Chiang, N. Bittner, Y. Pavlyukh, J. Berakdar, P. Werner, W. Widra, *Nat. Commun.* **2020**, *11*, 1 4095.
- [6] E. Perfetto, Y. Pavlyukh, G. Stefanucci, *Phys. Rev. Lett.* **2022**, *128*, 1 016801.
- [7] N. Schlünzen, J.-P. Joost, M. Bonitz, *Phys. Rev. Lett.* **2020**, *124*, 7 076601.
- [8] J.-P. Joost, N. Schlünzen, M. Bonitz, *Phys. Rev. B* **2020**, *101*, 24 245101.
- [9] Y. Pavlyukh, E. Perfetto, G. Stefanucci, *Phys. Rev. B* **2021**, *104*, 3 035124.
- [10] P. Lipavský, V. Špička, B. Velický, *Phys. Rev. B* **1986**, *34*, 10 6933.
- [11] Y. Pavlyukh, E. Perfetto, D. Karlsson, R. van Leeuwen, G. Stefanucci, *Phys. Rev. B* **2022**, *105*, 12 125134.
- [12] Y. Pavlyukh, E. Perfetto, D. Karlsson, R. van Leeuwen, G. Stefanucci, *Phys. Rev. B* **2022**, *105*, 12 125135.
- [13] D. Karlsson, R. van Leeuwen, Y. Pavlyukh, E. Perfetto, G. Stefanucci, *Phys. Rev. Lett.* **2021**, *127*, 3 036402.
- [14] R. Tuovinen, Y. Pavlyukh, E. Perfetto, G. Stefanucci, *Phys. Rev. Lett.* **2023**, *130*, 24 246301.
- [15] C. De Dominicis, P. C. Martin, *J. Math. Phys.* **1964**, *5*, 1 14.
- [16] K. Held, In E. Pavarini, E. Koch, D. Vollhardt, A. I. Lichtenstein, editors, *DMFT at 25: infinite dimensions: lecture notes of the Autumn School on Correlated Electrons 2014*. Forschungszentrum Jülich, Zentralbibliothek, Verl, Jülich, **2014**.
- [17] P. Romaniello, S. Guyot, L. Reining, *J. Chem. Phys.* **2009**, *131*, 15 154111.
- [18] D. J. Carrascal, J. Ferrer, J. C. Smith, K. Burke, *J. Phys. Condens. Matter* **2015**, *27*, 39 393001.
- [19] R. Mikhaylovskiy, E. Hendry, A. Secchi, J. Mentink, M. Eckstein, A. Wu, R. Pisarev, V. Kruglyak, M. Katsnelson, T. Rasing, A. Kimel, *Nat. Commun.* **2015**, *6*, 1 8190.
- [20] S. Di Sabatino, P.-F. Loos, P. Romaniello, *Frontiers in Chemistry* **2021**, *9* 751054.
- [21] J.-P. Joost, N. Schlünzen, H. Ohldag, M. Bonitz, F. Lackner, I. Březinová, *Phys. Rev. B* **2022**, *105*, 16 165155.
- [22] M. Berciu, *Phys. Rev. B* **2007**, *75*, 8 081101(R).
- [23] N. Säkkinen, Y. Peng, H. Appel, R. van Leeuwen, *J. Chem. Phys.* **2015**, *143*, 23 234102.
- [24] D. M. Kennes, E. Y. Wilner, D. R. Reichman, A. J. Millis, *Nature Phys.* **2017**, *13*, 5 479.
- [25] A. Bergschneider, V. M. Klinkhamer, J. H. Becher, R. Klemt, L. Palm, G. Zürn, S. Jochim, P. M. Preiss, *Nature Phys.* **2019**, *15*, 7 640.
- [26] K. S. Thygesen, *Phys. Rev. Lett.* **2008**, *100*, 16 166804.

- [27] M. P. v. Friesen, C. Verdozzi, C.-O. Almbladh, *J. Phys. Conf. Ser.* **2010**, 220 012016.
- [28] G. Stefanucci, R. van Leeuwen, *Nonequilibrium Many-Body Theory of Quantum Systems: A Modern Introduction*, Cambridge University Press, Cambridge, **2013**.
- [29] P. Romaniello, F. Bechstedt, L. Reining, *Phys. Rev. B* **2012**, 85, 15 155131.
- [30] Y. Pavlyukh, E. Perfetto, G. Stefanucci, *Phys. Rev. B* **2022**, 106, 20 L201408.
- [31] J. Yan, V. Janiš, *Phys. Rev. B* **2022**, 105, 8 085122.
- [32] G. Rohringer, A. Valli, A. Toschi, *Phys. Rev. B* **2012**, 86, 12 125114.
- [33] N. E. Bickers, D. J. Scalapino, *Ann. Phys.* **1989**, 193, 1 206.
- [34] V. Drchal, V. Janiš, J. Kudrnovský, V. S. Oudovenko, X. Dai, K. Haule, G. Kotliar, *J. Phys. Condens. Matter* **2005**, 17, 1 61.
- [35] N. E. Bickers, S. R. White, *Phys. Rev. B* **1991**, 43, 10 8044.